Carbohydrate Polymers 157 (2017) 503–511

Contents lists available at ScienceDirect

Carbohydrate Polymers

journal homepage: www.elsevier.com/locate/carbpol

Novel nanofibrillated cellulose/polyvinylpyrrolidone/silver nanoparticles films with electrical conductivity properties

Ahmed M. Khalil [a], Mohammad L. Hassan [b,c,*], Azza A. Ward [d]

[a] Photochemistry Department, National Research Centre, 33 El-Buhouth Street, Dokki, Giza 12622, Egypt
[b] Cellulose and Paper Department, National Research Centre, 33 El-Buhouth Street, Dokki, Giza 12622, Egypt
[c] Advanced Materials and Nanotechnology Group, Centre of Excellence for Advanced Sciences, National Research Centre, 33 El-Buhouth Street, Dokki, Giza 12622, Egypt
[d] Microwave Physics and Dielectrics Department, National Research Centre, 33 El-Buhouth Street, Dokki, Giza 12622, Egypt

ARTICLE INFO

Article history:
Received 16 June 2016
Received in revised form 4 October 2016
Accepted 4 October 2016
Available online 6 October 2016

Keywords:
Polyvinylpyrrolidone
Nanofibrillated cellulose
Rice straw
Silver nanoparticles
Electrical conductivity

ABSTRACT

Nanofibrillated cellulose (NFC) isolated from rice straw pulp was used with polyvinylpyrrolidone (PVP) and silver nanoparticles (AgNPs) to prepare nanocomposites in the form of flexible films. The later films have promising mechanical and electrical conductivity properties. The isolated cellulose nanofibers were characterized by transmission electron microscopy (TEM) and X-ray diffraction (XRD). Silver nanoparticles prepared via in-situ reduction in PVP were characterized using TEM and UV–vis spectroscopy. Tensile properties, microscopic structure, and electrical properties of nanocomposites films were studied. TEM and UV–vis spectroscopy proved the in-situ formation of AgNPs in PVP matrix. Films with good flexibility and tensile strength properties could be obtained from NFC/PVP/AgNPs as revealed from the (SEM) images and tensile properties testing. The electrical conductivity of NFC/PVP/AgNPs supports this system to be an excellent choice for sensitive electronic components packing as it can be used as antistatic and electrostatic dissipative materials.

1. Introduction

Nowadays, metal nanoparticles are considered as potential materials due to their various applications (Khalil et al., 2015; Rubilar et al., 2013; Stark, Stoessel, Wooleen, & Hafner, 2015) including electronics industry with their small size and precision of the electronic components. (Mishra, Dabrowski, Vij, Mishra, & Dhar, 2015; Park & Kim, 2014; Shen, Zhang, Huang, Xu, & Song 2014). Particularly, silver nanoparticles (AgNPs) have many applications; they can be used as antistatic materials, switching devices, conductive inks and adhesives for different electronics etc. . . (Bouvree, Feller, Castro, Grohens, & Rinaudo 2009; Deng et al., 2010; Thostenson & Chou, 2006). Various methods were used to synthesize metal nanoparticles including chemical, physical and thermal ones (Bae, Nam, & Park, 2002; Smetana, Klabunde, & Sorensen 2005). In addition, reduction either chemically, photochemically (Mallicka, Witcombb, & Scurrella, 2005) or electrochemically (Liu & Lin, 2004; Pinto et al., 2009) can be utilized. The chemical reduction method is one of the most common ones to prepare metal nanoparticles due to its simplicity, facility and abundance in production. Upon utilizing a strong reductant on silver nitrate in an aqueous reaction medium; such as sodium borohydride or hydrazine, silver nanoparticles (AgNPs) result from this process but a disadvantage may arise which is the aggregation of the aforementioned particles and losing their nanostructure. Silver nanoparticles can go through and combine with natural substrates as cotton and cellulosic materials. This can be achieved via reduction methods including the chemical or biological ones (Duran, Marcato, De Souza, Alves, & Esposito, 2007; Ravindra, Mohan, Reddy, & Raju, 2010). Polyvinylpyrrolidone (PVP) can be considered as an important ingredient in the synthesis of metal nanoparticles (MNPs). It has a role as a stabilizing agent in polar solvents and supports in determining the form of the prepared MNPs (Xia, Zeng, Zhang, Moran, & Xia, 2012). PVP has been utilized in preparing silver nanoparticles. These nanoparticles can disperse easily in PVP which in turn can act as protective layer around AgNPs preventing the aggregation that may occur (Zhang, Zhao, & Hu, 1996). Moreover, polyvinylpyrrolidone (PVP) performs an important role in the preparation of various composites (Zhao, Zhang, Du, Li, & Zou, 2015). It has been employed in preparing PVP/Fe_3O_4 (Wang, Li, Wang, & Wei, 2011). The effect of PVP was studied in investigating the electrical properties of polyacryloni-

* Corresponding author at: Cellulose and Paper Department, National Research Centre, 33 El-Buhouth Street, Dokki, Giza 12622, Egypt.
E-mail address: mlhassan2012@yahoo.com (M.L. Hassan).

http://dx.doi.org/10.1016/j.carbpol.2016.10.008
0144-8617/

trile (PAN) composite nanofibers combined with silver nitrate (Ucar et al., 2015). Hence, the aforementioned nanocomopsites loaded with PVP showed the ability to be used as antistatic materials.

Nanofibrillated cellulose (NFC) is an interesting natural-based polymeric material with unique properties such as ability for making transparent films with high tensile strength properties. There is a recent interest in using films from nanofibrillated cellulose in flexible electronics. Cellulose itself is a dielectric material and has been used for many years for this purpose. Rendering cellulose electrically conductive material adds a new functionality to it as well as new applications. This has been carried out by mixing it with nanostructured carbon (carbon nanotubes, graphene, reduced graphene oxide) (Deng et al., 2013; Salajkova, Valentini, Zhou, & Berglund, 2013; Zheng, Cai, Ma, & Gong, 2015), metal nanoparticles (Hao, Wang, Shao, & Yang, 2015;Yang & Li, 2015), conductive polymers, grafting its surface with conductive polymers (Jradi, Bideau, Chabot, & Daneault, 2012; Mattoso et al., 2009; Wang et al., 2016), or depositing a conducting material on the surface of cellulose (Wang et al., 2014). Mixing cellulose nanofibers with conductive polymers to prepare electrically conductive materials requires good compatibility between cellulose and the added polymer. Polyvinylpyrrolidone is a water soluble polymer and thus has excellent compatibility with cellulose. Although PVP films have perfect electrical conductivity properties but they suffer from low mechanical properties. Thus, nanocomposites containing cellulose nanofibers and PVP are able to produce novel materials with the unique properties extended from both of them. Surprisingly, few studies have been conducted so far on preparation of nanocomposites between cellulosic nanomaterials (cellulose nanocrystals or cellulose nanofibers) and PVP (Going, Sameoto, & Ayranci, 2015).

Conductive polymer composites (CPC) can be fabricated by adding conductive filler into polymer matrix. The most important advantage of CPC is that their electrical properties are close to those of fillers, even as their mechanical characteristics and processing are typical to plastics. Those composites have numerous benefits over the traditional conductive materials, inclusive processability, flexibility, light weight, ability to absorb mechanical shocks and low cost. CPC may be used as antistatic materials, switching devices, cables, transducers and gas sensors. Moreover, CPC can be employed as devices for electromagnetic radiation shielding and electrostatic discharge (Park, Thielemann, Asbeck, & Bandaru, 2010; Rashid, Ariffin, Akil, & Kooi, 2008; Liu et al., 2007). There are growing demands to decrease the thickness and diameter of conductive films. To preserve the processability of CPC with low cost, a minimum quantity of filler is mostly preferable. However by introducing an immiscible or partially miscible polymer to another one loaded with a conductive filler, a conductive polymer composite with minimal filler content can be obtained (Arbatti, Shan, & Cheng, 2007; Dang, Yu, Yao, & Liao, 2013).

The aim of this study is to utilize the flexibility and high tensile strength of nanofibrillated cellulose, electrical conductivity of PVP and silver nanoparticles in synthesizing nanocomposites in the forms of films with appropriate flexibility and tensile strength properties as well as electrical conductivity.

2. Materials and methods

2.1. Materials

Polyvinylpyrrolidone (PVP) with MW 1,300,000 was purchased from Alfa Aesar while silver nitrate (>99% $AgNO_3$) and sodium hydroxide (>97% NaOH) were from Sigma Aldrich. Rice straw was collected from local farms in Giza, Egypt. The used chemicals were of analytical grade. Deionized water was used to prepare the solutions.

2.2. Methods

2.2.1. Preparation of nanofibrillated cellulose (NFC)

Rice straw was washed, dried and chopped using a mill with a 1 cm wide sieve. To obtain cellulose pulp, 100 g rice straw was pulped using pulping mixture of 15% sodium hydroxide (based on wt. of rice straw) dissolved in 2 l of water at 150 °C for 2 h. The obtained pulp was washed to remove residual alkali and then bleached using sodium chlorite/acetic acid mixture according to the previously published method (Wise, Murphy, & D'Addieco, 1946). Chemical composition of the bleached pulp was determined according to the standard methods (Browning, 1967) being: Klason lignin 1.46%, alpha-cellulose 69.7%, hemicelluloses 19.7% and ash content 10.5%.

Bleached rice straw was first oxidized using (2,2,6,6-tetramethyl-1-piperidinyloxy) TEMPO; TEMPO/NaBr/sodium hypochlorite method as previously described (Hassan, Hassan, Abou-zeid, & El-Wakil, 2016) then subjected to high shear action using high-shear mixer at 10,000 rpm. The obtained gel was kept in the fridge till being used.

2.2.2. Preparation of silver nanoparticles (AgNPs)

Silver nanoparticles were prepared as previously described as follows (Sahoo et al., 2009): one gram of PVP was dissolved in 30 ml distilled water to prepare solution followed by adding 0.03 mol glucose and 0.01 mol of $AgNO_3$ at 65 °C with continuous stirring; pH was adjusted at 8.5–9 using 0.01 M sodium hydroxide. The molar ratio of glucose: silver nitrate was 1:2. The pH was maintained at 8.5–9 during the whole reaction. The reactants were heated at 65 °C for 30 min. After complete reduction of Ag^+ to Ag^0, acetone was used to precipitate the resulting nanoparticles coated with PVP. This was followed by repeated centrifugation for 20 min and washing with distilled water, dialyzed against distilled water, then dried under vacuum.

2.2.3. Preparation of PVP/NFC nanocpmposites

Nanofibrillated cellulose (NFC) suspension in water (1% wt%) was introduced into 5% aqueous solution of PVP. A series of solutions containing NFC/PVP (100/0, 75/25, 50/50 and 25/75 wt% based on oven dry weight) were prepared and poured into petri-dishes and dried in an oven at 40 °C for 24 h. The dried films with average thickness of about 0.08 mm were cut for characterizations and investigations.

2.2.4. Preparation of NFC/PVP/AgNPs nanocpmposites

The previous steps of preparing the NFC/PVP nanocomposites were followed by series of aqueous solutions containing NFC/PVP (100/0, 75/25, 50/50 and 25/75 wt%). A constant amount of coated silver nanoparticles of 2% wt% were introduced to PVP and nanofibrillated cellulose and stirred for 1 h producing nanocomposites suspension consisting of NFC/PVP/AgNPs (100/0/2, 75/25/2, 50/50/2, and 25/75/2 wt%). The prepared nanocomposites were poured into petri-dishes and dried in an oven at 40 °C for 24 h. Fig. 1 presents a schematic diagram for preparing the investigated nanocomposites at different concentrations of NFC/PVP/AgNPs. The thickness of the prepared films was about 0.08 mm.

2.3. Instrumentation

The transmission electron microscope (TEM) images of the colloidal nano-particles were attained using a JEOL JEM-2100 (JEOL, Japan). The TEM sample was prepared by mixing one dilute drop of prepared nanoparticles dispersed in acetone onto the copper grid and allowing it to dry well. The surface morphology of the examined sample was imaged with scanning electron microscope (SEM) (QUANTA FEG 250 ESEM). Energy dispersive X-ray spectroscopy

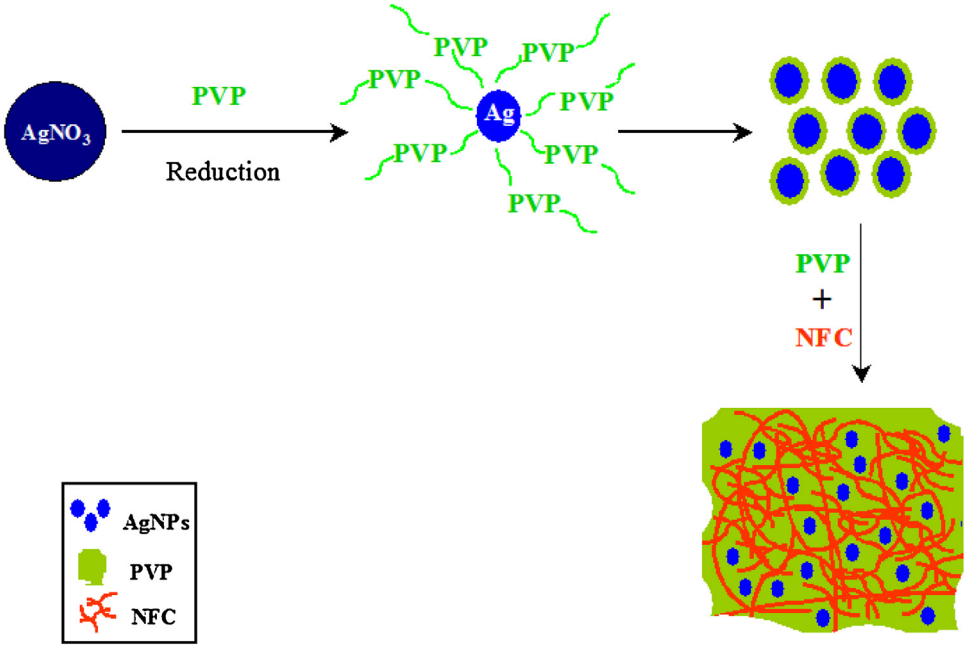

Fig. 1. Schematic diagram for preparing AgNPs coated with PVP and introducing them into NFC/PVP producing NFC/PVP/AgNPs nanocomposites at different polymeric concentrations.

(EDAX AMETEK Inc.; Mahwah, NJ, USA) analysis with acceleration voltage of 15 kV was carried out to determine elemental content. The dry sample was spread on a double sided conducting adhesive tape, pasted on a metallic stub. UV–vis absorption spectra were carried out for PVP and reduced silver ions producing coated silver nanoparticles with PVP. These spectra were for the diluted samples in deionized water performed by employing Agilent Cary 100 UV–vis Spectrometer. Diffraction pattern of nanofibrillated cellulose was obtained using Empyrean X-ray diffractometer (PANalytical, Netherlands). The diffraction pattern was recorded using Cu-Ka radiation at 40 kV and 25 mA. Tensile tests of nanocomposites films were carried out with a Lloyd instrument (LR10K; Lloyd Instruments, Fareham, UK) with a 100-N load cell. The measurements were performed at a crosshead speed of 2 mm/min at 25 °C.

Thermogravimetric analysis (TGA) was carried out using SDT Q600 Perkin-Elmer instrument (TA Instrument, USA) under nitrogen atmosphere with a heating rate of 10 °C/min and temperature from room temperature to 600 °C.

The conductivity measurements were carried out by means of high-resolution broadband impedance analyzer (Schlumberger Solartron 1260). Prepared films of known thickness *d* were placed between the electrodes of known area *A*. The measured conductance $G(\omega)$ from 0.1 Hz and 1 MHz was used to calculate conductivity $\sigma(\omega)$ using the following equation:

$$\sigma(\omega) = \frac{G(\omega) \times d}{A} \quad (1)$$

Perfect electromagnetic shielding was performed to the whole sample holder to decrease the general noise problems mainly at low frequencies. The measurements were automated by interfacing the impedance analyzer with a personal computer through a GPIB cable IEE488. An automation software Lab VIEW with a commercial interfacing was employed for acquisition of data. The error in conductance $G(\omega)$ amounts to 3%, respectively. The temperature of the samples was controlled by a temperature regulator with Pt 100 sensor having 0.5 °C as an error in temperature measurements. To avoid moisture, the samples were stored in desiccators containing silica gel. Then, the sample was transferred to the measuring cell and left with P_2O_5 until the measurements were performed.

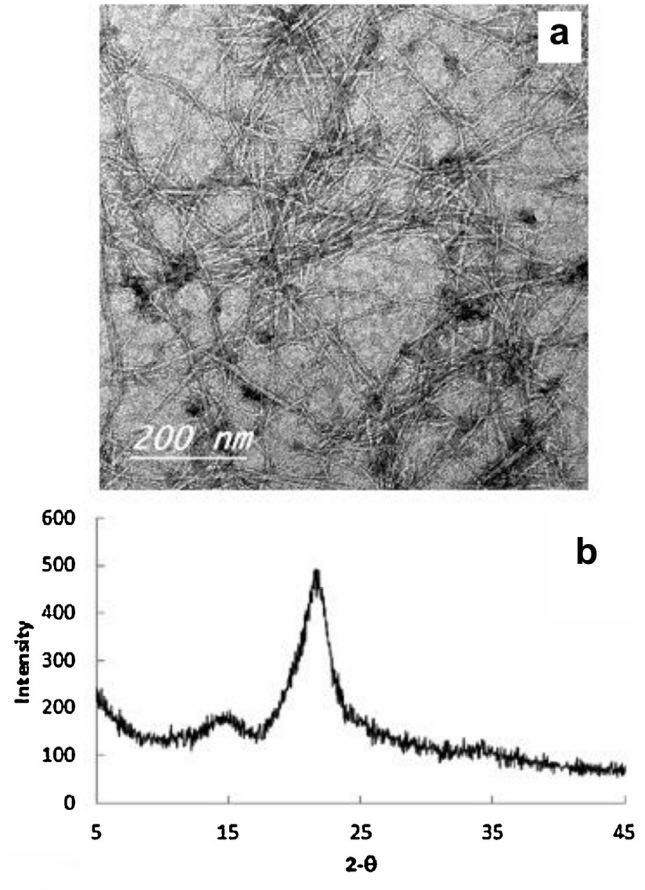

Fig. 2. (a) TEM image of nanofibrillated cellulose (NFC) (b) XRD of nanofibrillated cellulose (NFC).

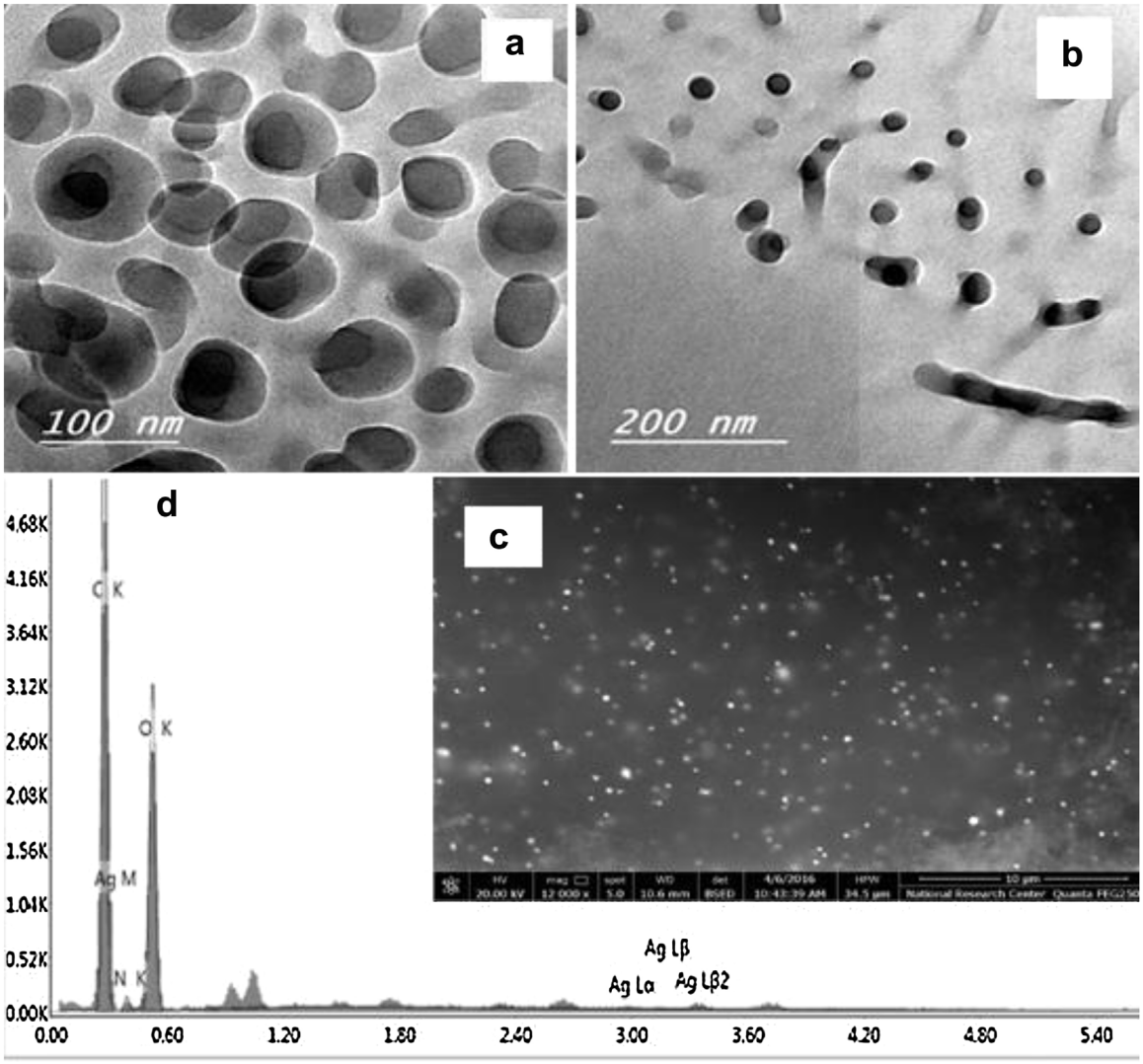

Fig. 3. (a) TEM images of a) AgNPs coated with PVP b) NFC/PVP/AgNPs nanocomposite (c &d) SEM and EDX images of NFC/PVP/AgNPs nanocomposite.

3. Results and discussion

3.1. Characterization of nanofibrillated cellulose (NFC)

TEM image in Fig. 2(a) for the isolated nanofibers shows homogenous width of about 4 nm and several microns in length. XRD diffraction pattern as illustrated in Fig. 2(b) of the NFC shows cellulose I structure with two characteristic peaks. Their values at 2θ are about 16° and 23° corresponding to the (101) and (002) crystallographic planes (Wada, Sugiyama, & Okano, 1993). The obtained XRD pattern is similar to that of cellulose nanofibers isolated from wood or wheat straw fibers by ultrasonic treatment (Chen et al., 2011).

3.2. Morphology of NFC/PVP/AgNPs nanocomposites

PVP was employed to prevent aggregation for the generated AgNPs. The mechanism of reduction of silver ions to silver nanoparticles in presence of PVP in aqueous solution could be explained similar to what was previously suggested as follows (Wang, Qiao, Chen, Wang, & Ding, 2005; Zhang, Zhao, and Lu, 1996). At first, a coordinative complex between silver ions and PVP is formed through donation loan pair electrons of oxygen and nitrogen atoms of PVP to S_p orbitals of silver. In the second step, PVP promotes the nucleation of the metallic silver reduced by glucose. Finally, PVP prohibits aggregation of silver particles and grain growth as a result of its steric effect. In Fig. 3(a), it is noticed that the diameter of the particles with dense color are about 25 nm, surrounded by PVP in lighter color. Silver nanoparticles were well dispersed with spherical structure. The presence of PVP prevented the agglomeration of these nanoparticles to larger particles. Upon preparing the NFC/PVP nanocomposite loaded with AgNPs as shown in Fig. 3(b); the previous structure can be noticed with a denser color surrounding the silver nanoparticles. This can be related to the PVP and nanofibrillated cellulose surrounding AgNPs. The morphology of NFC/PVP loaded with AgNPs was explored by scanning electron microscopy (SEM). Fig. 3(c) shows the fractured surface with homogeneity and compatibility between PVP and nanocellulose. In addition, the coated AgNPs with PVP are dispersed through the polymeric matrix. Fig. 3(d) illustrates energy dispersive X-ray spectroscopy (EDX) analysis for the investigated sample of NFC/PVP/AgNPs. It shows characteristic peaks for silver at 0.3 keV and in the vicinity of 3 keV with elemental composition of silver. Coating the silver nanoparticles with PVP led to weaken the peak of AgNPs. The latter observation can be related to the presence of PVP at this concentration 25% leading to an intensive polymeric structure (Malina, Sobczak-Kupiec, Wzorek, & Kowalski, 2012). Successively, this leads to weaken or prevent noticing the peak of silver nanopar-

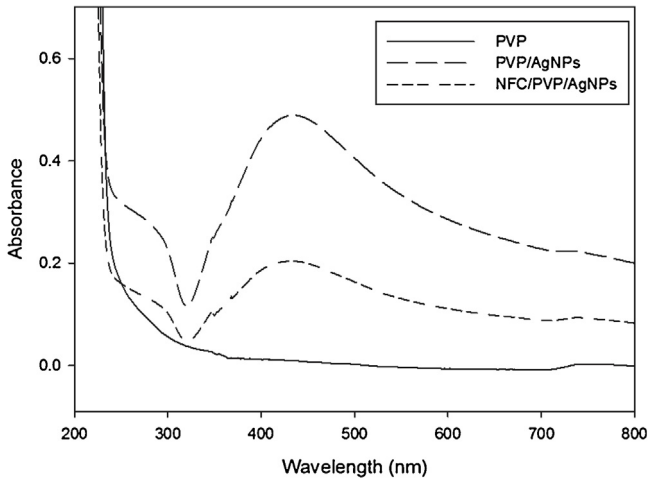

Fig. 4. UV–vis spectra of PVP, PVP/AgNPs, and NFC/PVP/AgNPs.

ticles. More peaks for C, N and O peaks appear in the spectrum presenting the other elements forming the investigated nanocomposite.

Fig. 4 illustrates the absorption spectra of PVP and AgNPs coated with PVP. The UV absorption spectrum of PVP does not show any distinctive peak. Nevertheless, PVP has an important role in coating the reduced silver ions into silver nanoparticles with expediting the reaction between $AgNO_3$ and glucose producing AgNPs with maintaining their uniformity. A noticeable absorption peak at 425 nm appears, confirming the presence of silver nanoparticles. Spherical silver nanoparticles have distinct UV absorption peak (Manna, Imae, Aoi, Okada, & Yogo, 2001; Pal, Tak, Song, 2007). Its maximum lies between 420 and 450 nm with some shifts depending on the size of the prepared nanoparticles. It was noted that addition of NFC to PVP/AgNPs resulted in shift of the peak at 425 nm to a lower wave length.

3.3. Tensile properties of NFC/PVP nanocomposites

Tensile properties of NFC/PVP and NFC/PVP/AgNPs nanocomposites are tested and shown in Fig. 5. Neat PVP films are very brittle and the tensile properties are difficult to be tested. Adding NFC to PVP makes it possible to prepare films with good mechanical properties and resulted in significant increase in tensile strength and modulus of PVP. This improvement is attributed to formation of network of NFC within PVP. However, increasing the percentage of NFC from 25% to 75% did not cause increase in tensile strength (maximum stress) but caused an increase in Young's modulus. This could be due to the high amount of NFC in the tested samples. Actually, using lower percentage of NFC than 25% with PVP did not result in films with good flexibility and tensile strength properties. It is noticed that there is a systematic decrease elongation% upon increasing the NFC in the investigated nanocomposites. In previous studies using NFC with different polymer matrices, the

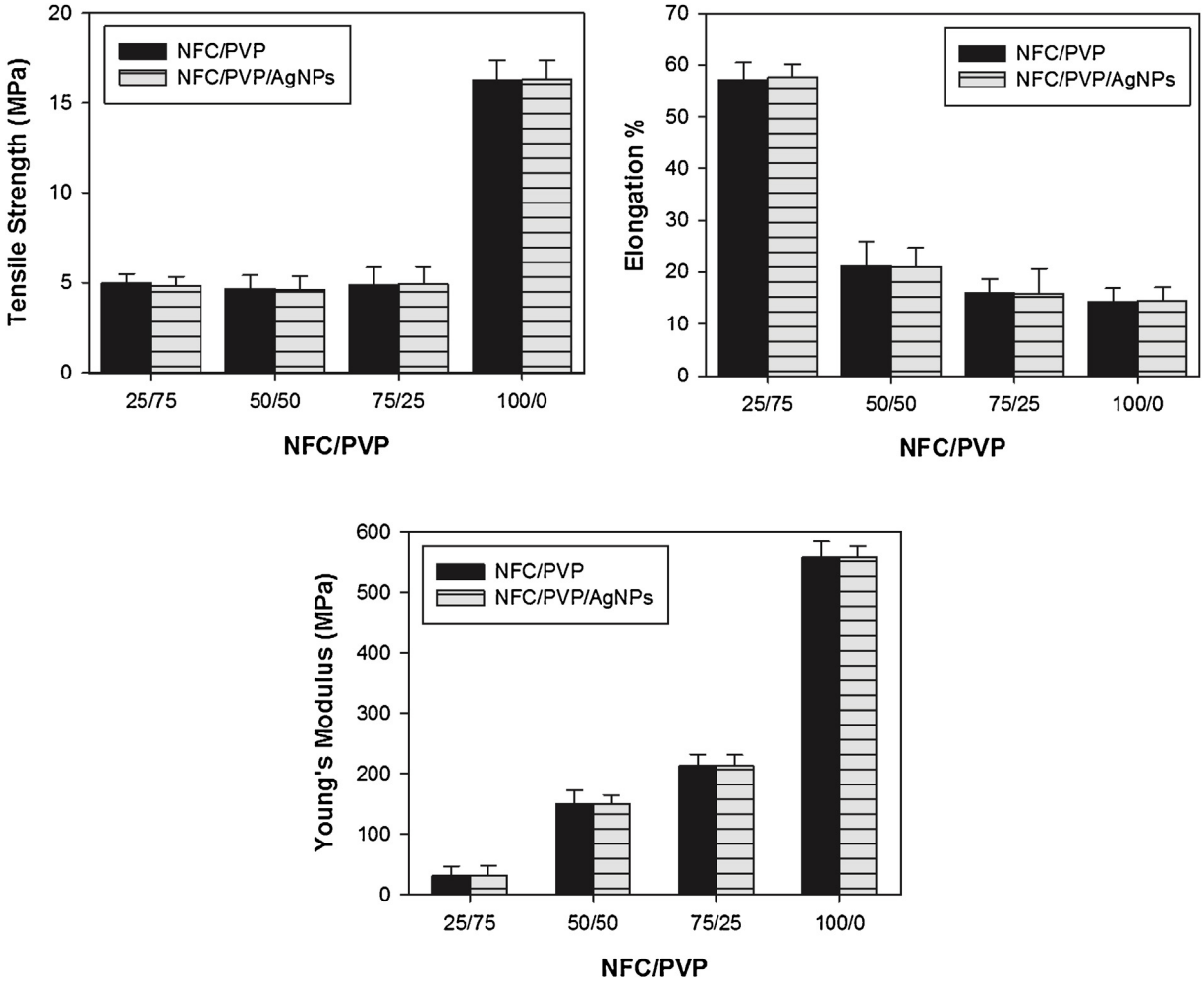

Fig. 5. Tensile properties of NFC/PVP and NFC/PVP/AgNPs nanocomposites.

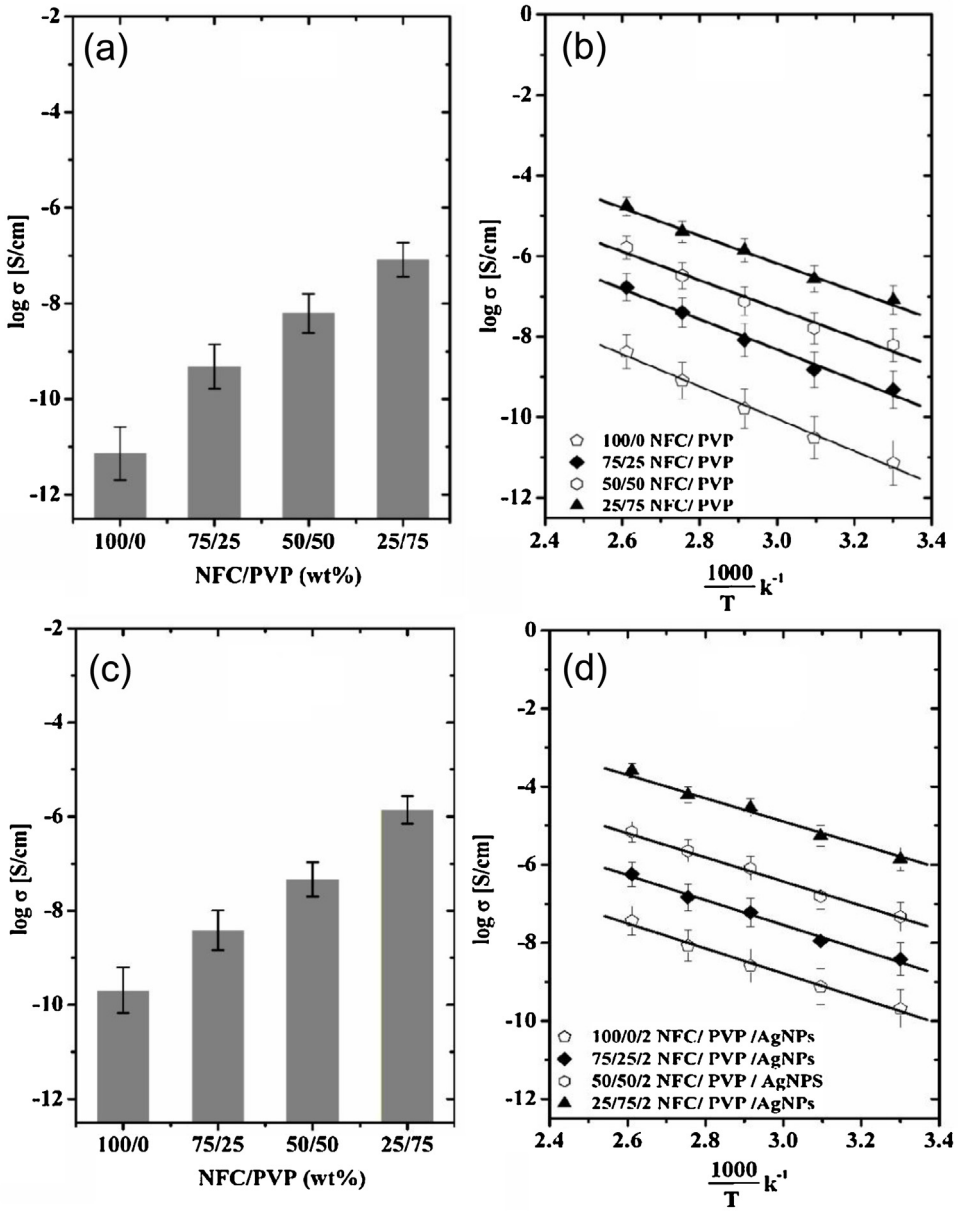

Fig. 6. (a) Conductivity versus NFC/PVP films at room temperature ~30 °C (b) Inverse temperature dependent conductivity of pure NFC and PVP films at different weight percent ratios (c) Conductivity versus NFC/PVP nanocomposites containing 2 (wt%) AgNPs at room temperature ~30 °C (d) Inverse temperature dependent conductivity of NFC/PVP nanocomposites containing 2 (wt%) AgNPs.

maximum improvement of tensile strength was achieved at relatively low percentage of NFC (less than the lowest ratio used in the current work) and no significant increase in tensile strength was achieved at higher loading of NFC (Feldman, 2015; Lee, Aitomaki, Berglund, Oksman, & Bismarck, 2014). Due to the higher stiffness of NFC than PVP, addition of NFC to PVP resulted in a decrease of elongation at break. Presence of AgNPs in the NFC/PVP films did not cause significant change in their mechanical properties.

3.4. Electrical conductivity of NFC/PVP/AgNPs nanocomposites

The electrical conductivities of the different polymeric ratios of NFC/PVP (100/0, 75/25, 50/50 and 25/75) at different temperatures are shown in Fig. 6(a). It is clear that the conductivity increased from 7.27×10^{-12} S/cm for pure NFC up to 8.23×10^{-8} S/cm at 30 °C when 75 wt% PVP was added. This increase in conductivity after addition of PVP can be attributed to the increase of the number of mobile charge carriers within the amorphous region of the polymer (Reffaee et al., 2014; Rozik, Khalaf, & Ward, 2016). The electrical conductivity boosts with elevating the temperature Fig. 6(b) and reaches its maximum value [1.73×10^{-5} S/cm] at 110 °C for 25/75 NFC/PVP. This can be explained by in terms of expansion of the amorphous region of the polymer which augments the segmental mobility of the polymeric chains. The increase in segmental mobility facilitated the ion migration resulting in higher conductivity (Williams, Landel, & Ferry, 1995).On the other hand, the conductivity of the nanocomposites 100/0/2, 75/25/2, 50/50/2 and 25/75/2 NFC/PVP/AgNPs versus the applied frequency at different temperatures is illustrated in Fig. 7. The total conductivity σ (ω) is nearly frequency independent at low frequency values, but is strongly frequency dependent at high frequency values for all NFC/PVP/AgNPs nanocomposites as can be seen in Fig. 7. Further, for all ratios under investigation,

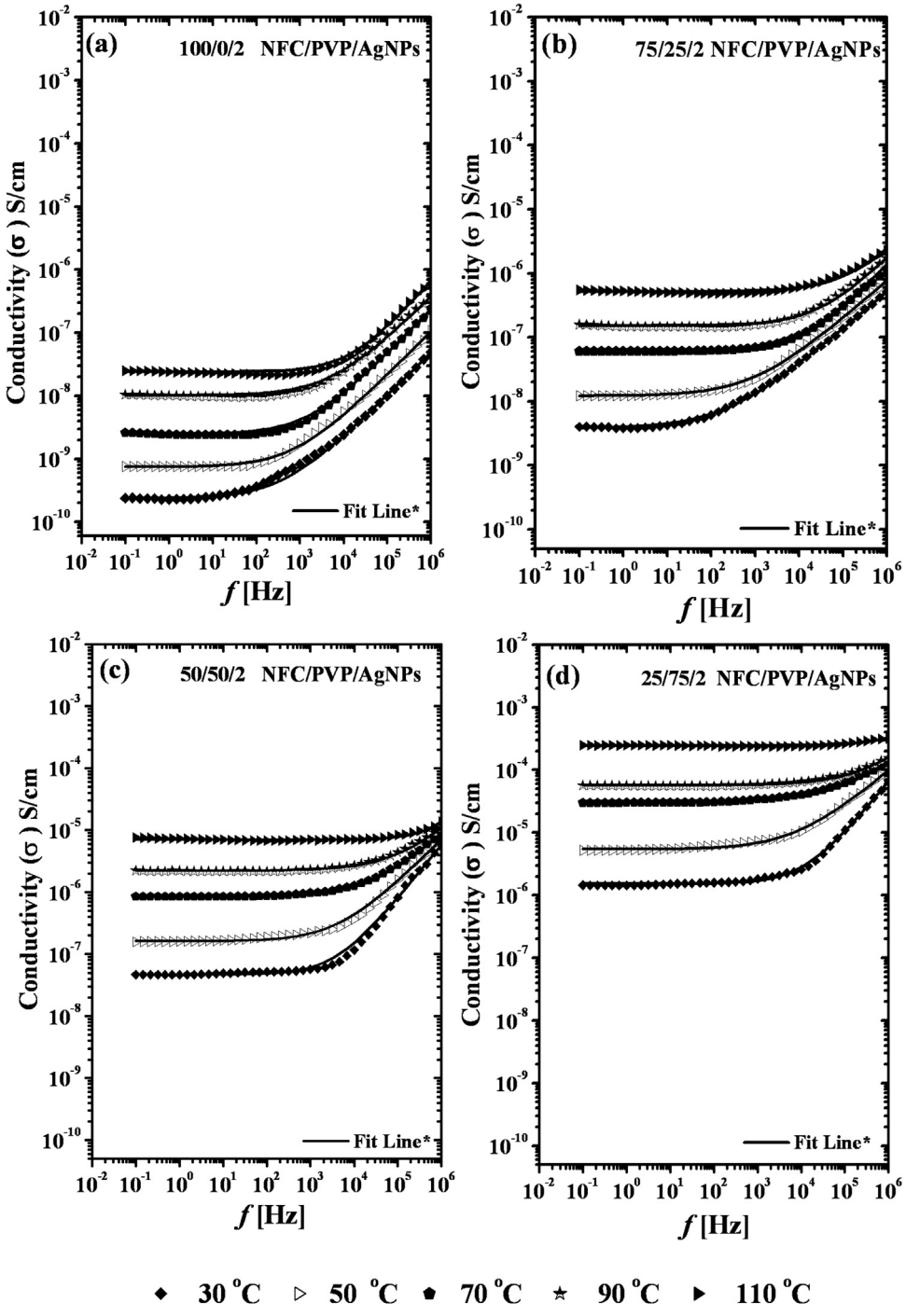

Fig. 7. Electrical conductivity of NFC/PVP/AgNPs nancomposites with various NFC/PVP ratios at fixed AgNPs content (2 wt%) and at different temperatures. * Fit line according to Eq. (3).

the conductivity obeys a power law relation in the high frequency range (Eq. (2);

$$\sigma(\omega) = A\omega^s \quad (2)$$

where ω is the angular frequency, A is a frequency independent parameter and *s* is a power (when $s \leq 1$, electronic hopping processes dominate). However, in the low frequency range (Hassan, Fadel, Ward, Moorefield, & Newkome, 2015; Masoud, Shaker, & Ali, 2006), the conductivity refers to the dc conductivity (σ_{dc}) giving by (Eq. (3)) (extrapolation of to σ (ω) to ω = 0).

$$\sigma(\omega) = \sigma_{dc} + A\omega^s \quad (3)$$

The progressive change from dc plateau to ac dispersive region indicates the distribution of relaxation times. The heterogeneity of the nanocomposites is the reason behind this distribution of relaxation times (Nassar, Ward, & Abdel Baseer, 2013). The total conductivity of PVP/NFC showed in Fig. 7 increases by addition of 2 wt% AgNPs. This increase is due to increase in the number of charge carriers and polarization effects (Khalaf & Ward, 2010).

In Fig. 6(c), the electrical conductivity values of the nanocomposites loaded with AgNPs, were improved compared to the values in Fig. 6(a) due to the presence of AgNPs. Moreover, these values changed from 2.36×10^{-10} S/cm for NFC/AgNPs to 1.5×10^{-6} S/cm for NFC/PVP/AgNPs 25/75/2 at room temperature (~30 °C). These

Table 1
Activation energy for ionic conductivity of NFC/PVP/AgNPs nanocomposites films.

NFC/PVP	Activation energy (eV)[a]	NFC/PVP/AgNPs	Activation energy (eV)[b]
100/0	0.335	100/0/2	0.286
75/25	0.315	75/25/2	0.272
50/50	0.294	50/50/2	0.263
25/75	0.273	25/75/2	0.242

[a]Calculated from Fig. 6b.
[b] Calculated from Fig. 6d.

results highly recommend NFC/PVP/AgNPs nanocomposites to be utilized as antistatic and electrostatic dissipative materials. This makes it an excellent choice for sensitive electronic components as the suitable range of conductivity for such applications is 10^{-12}–10^{-10} S/cm for antistatic whereas for electrostatic dissipation (ESD) applications the range is 10^{-9}–10^{-5} S/cm respectively (Skotheim, 1997). Hence, these materials can be used in conjunction with other electrostatic dissipation (ESD) materials to remove the discharge or sparks and good for clean rooms on the floor as they contain silver.

The variance of log (σ) as a function of inverse absolute temperature for PVP/NFC/AgNPs nanocomposites is shown in Fig. 6(d). From this figure, it is observed that the values of electrical conductivities for the tested samples increased with elevating the temperature. The aforementioned results coincide with the free volume theory (Linford, 1987; Skotheim, 1997). Upon increasing the temperature, the amorphous region of the polymer can expand easily, resulting in a boosting free volume of the system. Consequently, the segmental motion allows the ions to leap from one site to another or supplies a pathway for mobilizing the ions. Moreover, the segmental movement of the polymer facilitates the translational ionic motion. Thus an increase in temperature produces more free volumes, which increases the mobility of ions and hence conductivity (Ramesh, Yahana, & Arof, 2002).

However, Fig. 6(b) and (d) reveal that the conductivity (σ) does not show any sudden change with the temperature. This indicates that the samples reveal an amorphous nature. A linear dependence obtained in Fig. 6(b) and (d) is noticed suggesting that the ion conduction follows Arrhenius behavior (Gad, Moustafa, & Ward, 2015; Ramesh & Ng, 2009) and the results may be represented by the following Eq. (4):

$$\sigma = \sigma_o \ \exp\left[\frac{-Ec}{kT}\right] \quad (4)$$

where σ_o is the pre-exponential term, k is the Boltzmann constant and E_c is the activation energy. The values of the calculated activation energy from the slopes of linear fit of Arrhenius plots Fig. 6(b) and (d) are listed in Table 1. However, the values of activation energy listed in aforementioned table represent the required energy for the motion of charge carriers. Moreover, the activation energy is found to decrease gradually with increasing PVP content and the presence of AgNPs confirming the increase in amorphous nature of the polymeric matrix.

It should be pointed out that the prepared NFC by TEMPO oxidation is known to have thermal stability up to 200 °C (Hassan & Hassan, 2016) while PVP has thermal stability up to 380 °C (Du et al., 2006). The TGA curves of NFC and PVP/AgNPs used in the current work (Fig. S1) showed thermal stability (onset degradation temperature) of about 215 °C and 390 °C, respectively.

4. Conclusions

Flexible films from nanofibrillated cellulose (NFC) and polyvinylpyrrolidone (PVP) in absences and presence of silver nanoparticles (AgNPs) were prepared. Mechanical properties, microscopic structure and electrical properties of nanocomposites films were investigated using tensile testing, scanning electron microscopy (SEM), and high-resolution broad band impedance analyzer, respectively. The loaded nanocomposites with AgNPs showed promising electrical conductivity for various applications. The prepared films may be used as antistatic and static dissipative materials. The prepared nanocomposites films showed good homogeneity and acceptable tensile strength properties. Among different concentrations of the investigated nanocomopsites, NFC/PVP/AgNPs 25/75/2 showed the highest electrical conductivity. The electrical conductivity of NFC/PVP/AgNPs nanocomposites was within the range of (2.36×10^{-10} S/cm–1.5×10^{-6} S/cm) at 30 °C. This supports the prepared nanocomposites films to be an excellent choice for sensitive electronic packing components.

Acknowledgment

The authors gratefully acknowledge the National Research Centre (NRC) – Egypt for financial support through Project no. 10130103 entitled “Preparation of cellulosic nanomaterials from rice straw and their use to improve locally produced paper products”, 2013–2016.

Appendix A. Supplementary data

Supplementary data associated with this article can be found, in the online version, at 10.1016/j.carbpol.2016.10.008.

References

Arbatti, M., Shan, X. B., Cheng, & ZY. (2007). Ceramic–polymer composites with high dielectric constant. *Advanced Materials*, *1199*, 1369–1372.
Bae, C. H., Nam, S. H., & Park, S. M. (2002). Formation of silver nanoparticles by laser ablation of a silver target in NaCl solution. *Applied Surface Science*, *197–198*, 628–634.
Bouvree, A., Feller, J.-F., Castro, M., Grohens, Y., & Rinaudo, M. (2009). Conductive polymer nano-bioComposites (CPC): Chitosan-carbon nanoparticle a good candidate to design polar vapour sensors. *Sensors and Actuators B: Chemical*, *138*, 138–147.
Browning, B. L. (1967). . *Methods of wood chemistry* (Vol. 2) New York: Interscience.
Chen, W., Yu, H., Liu, Y., Hai, Y., Zhang, M., & Chen, P. (2011). Isolation and characterization of cellulose nanofibers from four plant cellulose fibers using a chemical-ultrasonic process. *Cellulose*, *18*, 433–442.
Dang, Z. M., Yu, J. K., Yao, S. H., & Liao, R. J. (2013). Flexible nanodielectric materials with high permittivity for power energy storage. *Advanced Materials*, *25*, 6334–6365.
Deng, H., Skipa, T., Bilotti, E., Zhang, R., Lellinger, D., Mezzo, L., . . . & Peijs, T. (2010). Preparation of high performance conductive polymer fibers through morphological control of networks formed by nanofillers. *Advanced Functional Materials*, *20*, 1424–1432.
Deng, L., Young, R. J., Kinloch, I. A., Abdelkader, A. M., Holmes, S. M., De Haro-Del Rio, D. A., & Eichhorn, S. J. (2013). Supercapacitance from cellulose and carbon nanotube nanocomposite fibers. *ACS Applied Materials and Interfaces*, *5*, 9983–9990.
Du, Y. K., Yang, P., Mou, Z. G., Hua, N. P., & Jiang, L. (2006). Thermal decomposition behaviors of PVP coated on platinum nanoparticles. *Journal of Applied Polymer Science*, *99*, 23–26.
Duran, N., Marcato, P. D., De Souza, G. I. H., Alves, O. L., & Esposito, E. (2007). Antibacterial effect of silver nanoparticles produced by fungal process on textile fabrics and their effluent treatment. *Journal of Biomedical Nanotechnology*, *3*, 203–208.
Feldman, D. (2015). Cellulose nanocomposites (2015). *Journal of Macromolecular Science, Part A: Pure and Applied Chemistry*, *52*, 322–329.
Gad, S. A., Moustafa, A. M., & Ward, A. A. (2015). Preparation and some physical properties of $Zn_{1-x}Cr_xO$. *Journal of Inorganic and Organometallic Polymers and Materials*, *25*, 1077–1087.
Going, R. J., Sameoto, D. E., & Ayranci, C. (2015). Cellulose nanocrystals: Dispersion in co-solvent systems and effects on electrospun polyvinylpyrrolidone fiber mats. *Journal of Engineered Fibers and Fabrics*, *10*, 155–163.
Hao, H., Wang, X., Shao, Z., & Yang, R. (2015). Transparent flexible conductive thin films based on cellulose nanofibers by layer-by-layer assembly method and its fabricated electrochromic flexible supercapacitors. *Chemical Journal of Chinese Universities*, *36*, 1838–1845.
Hassan, E. A., & Hassan, M. L. (2016). Rice straw nanofibrillated cellulose films with antimicrobial properties via supramolecular rout. *Industrial Crops and Products*, *93*, 142–151.
Hassan, M. L., Fadel, S. M., Ward, A. A., Moorefield, C. M., & Newkome, G. R. (2015). Electrical properties of FeII-terpyridine-modified cellulose nanocrystals and

polycaprolactone/FeII-CTP nanocomposites. *Polymer Composites*, http://dx.doi.org/10.1002/pc.23468
Hassan, E. A., Hassan, M. L., Abou-zeid, R. E., & El-Wakil, N. A. (2016). Novel nanofibrillated cellulose/chitosan nanoparticles nanocomposites films and their use for paper coating. *Industrial Crops and Products*, *93*, 219–226.
Jradi, K., Bideau, B., Chabot, B., & Daneault, C. (2012). Characterization of conductive composite films based on TEMPO-oxidized cellulose nanofibers and polypyrrole. *Journal of Materials Science*, *47*, 3752–3762.
Khalaf, A. I., & Ward, A. A. (2010). Use of rice husks as potential filler in styrene butadiene rubber/linear low density polyethylene blends in the presence of maleic anhydride. *Materials and Design*, *31*, 2414–2421.
Khalil, A. M., Georgiadou, V., Guerrouache, M., Mahouche-Chergui, S., Dendrinou-Samara, C., Chehimi, M. M., & Carbonnier, B. (2015). Gold-decorated polymeric monoliths: In-situ vs ex-situ immobilization strategies and flow through catalytic applications towards nitrophenols reduction. *Polymer*, *77*, 218–226.
Lee, K., Aitomaki, Y., Berglund, L. A., Oksman, K., & Bismarck, A. (2014). On the use of nanocellulose as reinforcement in polymer matrix composites. *Composites Science and Technology*, *105*, 15–27.
Linford, R. G. (1987). *Electrochemical science and technology of polymers*. London: Elsevier Applied Science.
Liu, Y. C., & Lin, L. H. (2004). New pathway for the synthesis of ultrafine silver nanoparticles from bulk silver substrates in aqueous solutions by sonoelectrochemical methods. *Electrochemistry Communications*, *6*, 1163–1168.
Liu, Z., Bai, G., Huang, Y., Li, F., Ma, Y., Guo, T., . . . & Chen, Y. (2007). Microwave absorption of single-walled carbon nanotubes/soluble cross-linked polyurethane composites. *The Journal of Physical Chemistry C*, *111*, 13696–13700.
Malina, D., Sobczak-Kupiec, A., Wzorek, Z., & Kowalski, Z. (2012). Silver nanoparticles synthesis with different concentrations of Polyvinylpyrrolidone. *Digest Journal of Nanomaterials and Biostructures*, *7*, 1527–1534.
Mallicka, K., Witcombb, M. J., & Scurrella, M. S. (2005). Self-assembly of silver nanoparticles in a polymer solvent: Formation of a nanochain through nanoscale soldering. *Materials Chemistry and Physics*, *90*, 221–224.
Manna, A., Imae, T., Aoi, K., Okada, M., & Yogo, T. (2001). Synthesis of dendrimer-passivated noble metal nanoparticles in a polar medium: Comparison of size between silver and gold particles. *Chemistry of Materials*, *13*, 1674–1681.
Masoud, M. S., Shaker, M. A., & Ali, A. E. (2006). Dielectric spectroscopy of some heteronuclear amino alcohol complexes. *Spectrochimica Acta Part A*, *65*, 127–132.
Mattoso, L. H. C., Medeiros, E. S., Baker, D. A., Avloni, J., Wood, D. F., & Orts, W. J. (2009). Electrically conductive nanocomposites made from cellulose nanofibrils and polyaniline. *Journal of Nanoscience and Nanotechnology*, *9*, 2917–2922.
Mishra, M., Dabrowski, R. S., Vij, J. K., Mishra, A., & Dhar, R. (2015). Electrical and electro-optical parameters of 4′-octyl-4-cyanobiphenyl nematic liquid crystal dispersed with gold and silver nanoparticles. *Liquid Crystals*, *42*, 1580–1590.
Nassar, M. A., Ward, A. A., & Abdel Baseer, R. (2013). Synthesis and characterization of polyaniline nanocomposites. *Kautschuk Gummi Kunststoffe*, *66*, 39–46.
Pal, S., Tak, Y. K., & Song, J. M. (2007). Does the antibacterial activity of silver nanoparticles depend on the shape of the nanoparticle? A study of the Gram-negative bacterium Escherichia coli. *Applied and Environmental Microbiology*, *73*, 1712–1720.
Park, S., & Kim, H. (2014). Flash light sintering of nickel nanoparticles for printed electronics. *Thin Solid Films*, *500*, 575–581.
Park, S. H., Thielemann, P. T., Asbeck, P. S., & Bandaru, P. R. (2010). Enhanced electromagnetic interference shielding through the use of functionalized carbon-nanotube-reactive polymer composites. *IEEE Transactions on Nanotechnology*, *9*, 464–469.
Pinto, R. J. B., Marques, P. A. A. P., Neto, C. P., Trindade, T., Daina, S., & Sadocco, P. (2009). Antibacterial activity of nanocomposites of silver and bacterial or vegetable cellulosic fibers. *Acta Biomaterialia*, *5*, 2279–2289.
Ramesh, S., & Ng, K. Y. (2009). Characterization of polymer electrolytes based on high molecular weight PVC and Li_2SO_4. *Current Applied Physics*, *9*, 329–332.
Ramesh, S., Yahana, A. H., & Arof, A. K. (2002). Dielectric behaviour of PVC-based polymer electrolytes. *Solid State Ionics*, *152*, 291–294.
Rashid, E. S. A., Ariffin, K., Akil, H. M., & Kooi, C. C. (2008). Mechanical and thermal properties of polymer composites for electronic packaging application. *Journal of Reinforced Plastics and Composites*, *27*, 1573–1584.
Ravindra, S., Mohan, Y. M., Reddy, N. N., & Raju, K. M. (2010). Fabrication of antibacterial cotton fibres loaded with silver nanoparticles via 'Green approach'. *Colloids and Surfaces A: Physicochemical and Engineering Aspects*, *367*, 31–40.
Reffaee, A. A., Ward, A. A., El-Nashar, D. E., Abd-El-Messieh, S. L., Abdel Nour, K. N., Gomaa, E., & Zayed, H. A. (2014). Dielectric properties and positron annihilation study of waste polyethylene terephthalate composites filled with carbon black. *Kautschuk Gummi Kunststoffe*, *67*, 39–47.
Rozik, N. N., Khalaf, A. I., & Ward, A. A. (2016). Studies the behaviors of polyaniline on the properties of PS/PMMA blends. *Proceedings of the Institution of Mechanical Engineers, Part L: Journal of Materials: Design and Applications*, *230*, 526–553.
Rubilar, O., Rai, M., Tortella, G., Diez, M. C., Seabra, A. B., & Duran, N. (2013). Biogenic nanoparticles: Copper, copper oxides, copper sulphides, complex copper nanostructures and their applications. *Biotechnology Letters*, *35*, 1365–1375.
Sahoo, P. K., Kamal, S. S., Jagadeesh, T., Sreedhar, B., Singh, A. K., & Srivastava, S. K. (2009). Synthesis of silver nanoparticles using facile wet chemical route. *Defence Science Journal*, *59*, 447–455.
Salajkova, M., Valentini, L., Zhou, Q., & Berglund, L. A. (2013). Tough nanopaper structures based on cellulose nanofibers and carbon nanotubes. *Composites Science and Technology*, *87*, 103–110.
Shen, W., Zhang, X., Huang, Q., Xu, Q., & Song, W. (2014). Preparation of solid silver nanoparticles for inkjet printed flexible electronics with high conductivity. *Nanoscale*, *6*, 1622–1628.
Skotheim, T. A. (1997). *Handbook of conducting polymers* (2nd ed.). CRC Press.
Smetana, A. B., Klabunde, K. J., & Sorensen, C. M. (2005). Synthesis of spherical silver nanoparticles by digestive ripening, stabilization with various agents, and their 3-D and 2-D superlattice formation. *Journal of Colloid and Interface Science*, *284*, 521–526.
Stark, W. J., Stoessel, P. R., Wooleen, W., & Hafner, A. (2015). Industrial applications of nanoparticles. *Chemical Society Reviews*, *44*, 5793–5805.
Thostenson, E. T., & Chou, T. W. (2006). Carbon nanotube networks: Sensing of distributed strain and damage for life prediction and self healing. *Advanced Materials*, *18*, 2837–2841.
Ucar, N., Demirsoy, N., Onen, A., Karacan, I., Kizildag, N., Eren, O., . . . & Ustamehmetoglu, B. (2015). The effect of reduction methods and stabilizer (PVP) on the properties of polyacrylonitrile (PAN) composite nanofibers in the presence of nanosilver. *Journal of Materials Science*, *50*, 1855–1864.
Wada, M., Sugiyama, J., & Okano, T. (1993). Native celluloses on the basis of two crystalline phase (I-alpha/I-beta) system. *Journal of Applied Polymer Science*, *49*, 1491–1496.
Wang, H., Qiao, X., Chen, J., Wang, X., & Ding, S. (2005). Mechanisms of PVP in the preparation of silver nanoparticles. *Materials Chemistry and Physics*, *94*, 449–453.
Wang, X., Li, X. J., Wang, Q. Q., & Wei, Q. F. (2011). Preparation and characterization of PVP/Fe_3O_4 composite nanofibers. *Advanced Materials Research*, *332–334*, 783–786.
Wang, X., Gao, K., Shao, Z., Peng, X., Wu, X., & Wang, F. (2014). Layer-by-layer assembled hybrid multilayer thin film electrodes based on transparent cellulose nanofibers paper for flexible supercapacitors applications. *Journal of Power Sources*, *249*, 148–155.
Wang, S., Wei, C., Gong, Y., Lv, J., Yu, C., & Yu, J. (2016). Cellulose nanofiber-assisted dispersion of cellulose nanocrystals@polyaniline in water and its conductive films. *RSC Advances*, *6*, 10168–10174.
Williams, M. L., Landel, R. F., & Ferry, J. D. (1995). The temperature dependence of relaxation mechanisms in amorphous polymers and other glass-forming liquids. *Journal of American Chemical Society*, *77*, 3701–3707.
Wise, L. E., Murphy, M., & D'Addieco, A. A. (1946). Chlorite holocellulose, its fractionation and bearing on summative wood analysis and on studies on hemicelluloses. *Paper Trade Journal*, *122*, 35–43.
Xia, X., Zeng, J., Zhang, Q., Moran, C., & Xia, Y. (2012). Recent developments in shape-controlled synthesis of silver nanocrystals. *The Journal of Physical Chemistry C*, *116*, 21647–21656.
Yang, C., & Li, D. (2015). Flexible and foldable supercapacitor electrodes from the porous 3D network of cellulose nanofibers, carbon nanotubes and polyaniline. *Materials Letters*, *155*, 78–81.
Zhang, Z., Zhao, B., & Hu, L. (1996). PVP protective mechanism of ultrafine silver powder synthesized by chemical reduction processes. *Journal of Solid State Chemistry*, *121*, 105–110.
Zhao, T., Zhang, C., Du, Z., Li, H., & Zou, W. (2015). Functionalization of AgNWs with amino groups and their application in an epoxy matrix for antistatic and thermally conductive nanocomposites. *RSC Advances*, *5*, 91516–91523.
Zheng, Q., Cai, Z., Ma, Z., & Gong, S. (2015). Cellulose nanofibril/reduced graphene oxide/carbon nanotube hybrid aerogels for highly flexible and all-solid-state supercapacitors. *ACS Applied Materials and Interfaces*, *7*, 3263–3271.